XAM17

XP-002282688

IEEE PHOTONICS TECHNOLOGY LETTERS, VOL. 15, NO. 7, JULY 2003

Side Detection of Strong Radiation-Mode Out-Coupling From Blazed FBGs in Single-Mode and Multimode Fibers

P.D. 07-2003
p. 936-938 3

K. Zhou, A. G. Simpson, L. Zhang, and I. Bennion

Abstract—We report on the effective side detection of radiation-mode out-coupling from blazed fiber Bragg gratings (BFBGs) fabricated in single-mode fiber (SMF) and multimode fiber (MMF). The far-field radiation power distribution from BFBGs have been measured achieving a high spatial–spectral resolution (0.17 mm/nm). We have also investigated comparatively the transmission-loss characteristics of BFBGs in both fiber types, fabricated using phase-mask and holographic inscription techniques. Our results reveal clearly that the radiation out-coupling from BFBGs is significantly stronger and spectrally more confined in MMF than in SMF.

Index Terms—Blazed fiber Bragg gratings (BFBGs), multimode fibers (MMFs), radiation-mode out-coupling, single-mode fibers (SMFs).

I. Introduction

MOST FIBER Bragg grating (FBG) applications utilize coupling between forward and backward propagating core modes. Different mode couplings exist, such as core-cladding and core-radiation coupling, which are usually associated with long-period and blazed (or tilted) grating structures, respectively. Radiation-mode out-coupling from blazed FBGs (BFBGs) has already been demonstrated for applications in wavelength-division-multiplexing (WDM) channel monitoring [1], gain flattening of erbium-doped fiber amplifiers [2], polarization discrimination [3], and optical sensor interrogation [4]; there are, however, very few reports to date on the side detection of radiation modes at the grating's location within the fiber. Side detection of radiation modes offers many application-specific advantages; for example, in conjunction with a charged-coupled device array detector, the function of side-tapping light with high spectral resolution from BFBGs may be utilized to implement a spectrometer function or to form the basis of low-cost WDM devices. In this letter, we report for the first time to our knowledge, the effective side detection of radiation-mode profiles of BFBGs fabricated in single-mode fiber (SMF) and multimode fiber (MMF). We have comparatively investigated the radiation-mode out-coupling characteristics of BFBGs in both fiber types fabricated using phase-mask and holographic inscription techniques.

Manuscript received November 13, 2002; revised March 11, 2003. This work was supported by the U.K. DTI-EPSRC LINK under Project EMPIRE.

The authors are with the Photonics Research Group, Electronic Engineering, Aston University, Birmingham, B4 7ET, U.K.

Digital Object Identifier 10.1109/LPT.2003.813568

II. Characteristics of Transmission-Loss Profiles of BFBGs

BFBGs may be ultraviolet (UV)-inscribed using the phase-mask or the holographic interference techniques. Fringes in BFBGs are slanted either by tilting the mask with respect to the fiber or by rotating the fiber in the plane formed by the two interfering beams. Considering the geometrical arrangements in the two fabrication systems [5], [6] and applying the phase match conditions for Bragg reflection and radiation-mode out-coupling [7]

$$\overrightarrow{K_B} = \overrightarrow{K_{\rm in}} + \overrightarrow{K_G} \tag{1}$$

$$\overrightarrow{K_R} = \overrightarrow{K_{\rm in}} + \overrightarrow{K'_G} \tag{2}$$

where $\overrightarrow{K_B}$ and $\overrightarrow{K_R}$ are the Bragg and radiation-mode wave vectors, respectively, $\overrightarrow{K_{\rm in}}$ is the wave vector of incident light, and $\overrightarrow{K_G}(K_G = 2\pi/\Lambda_G)$ and $\overrightarrow{K'_G}(K'_G = 2\pi/(\Lambda_G \cos\theta_{\rm int}))$ are the grating wave vectors; we can plot the relationship between the Bragg and radiation responses and the external tilting angles of the fiber, as shown in Fig. 1(d). Two trends can be clearly seen from Fig. 1(d): with increasing tilt angle, 1) the Bragg response shifts nonlinearly toward longer wavelengths at a much higher rate for the BFBGs fabricated using the holographic method than that using the phase-mask technique; 2) the radiation responses of gratings fabricated using both methods shift in opposite directions with a similar rate.

In order to examine the characteristics of the radiation-mode out-coupling, BFBGs were UV-inscribed in standard telecom H_2-loaded SMF and MMF by both phase-mask and holographic techniques. The tilt angles for gratings written by the phase-mask method were limited by the narrow width of the mask's fringe patterns to 6° whereas the holographic setup yielded up to 20°.

Fig. 2(a) and (b) shows the transmission spectra for two sets of BFBGs fabricated in SMF by the phase-mask and holographic methods, respectively. The transmission-loss characteristics are clearly related to tilt angle by Fig. 2, wherein it is further demonstrated that with increasing tilt angle, the Bragg resonance shifts toward longer wavelengths while its strength decreases. The radiation-mode out-coupling (appearing as a broad transmission-loss peak) also evolves as its strength decreases and dynamic range increases when the fringes are more slanted. However, it is noted that the wavelengths at

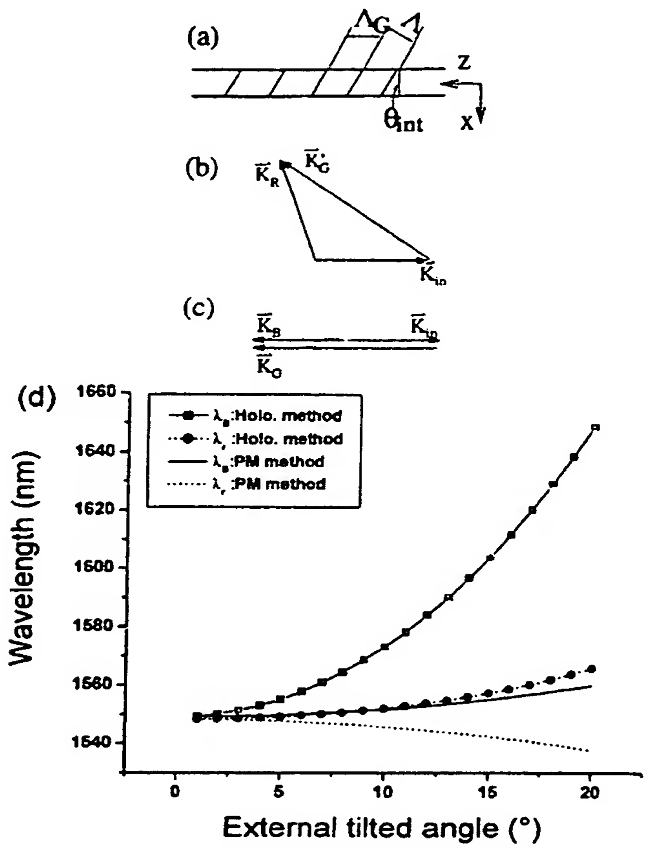

Fig. 1. (a) Geometry of a BFBG; wave vector relationships for (b) radiation and (c) Bragg phase match conditions. (d) Calculated relationship between Bragg and radiation wavelengths and external tilt angles for BFBGs realized using phase-mask and holographic methods.

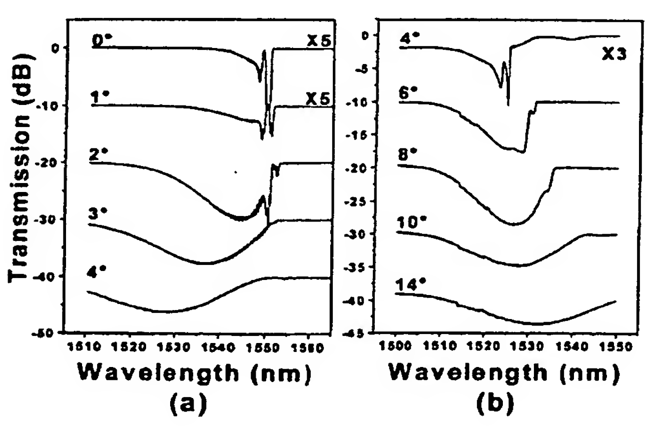

Fig. 2. Transmission-loss profiles of two sets of BFBGs in SMF fabricated using (a) phase-mask and (b) holographic techniques. Note: the top two curves in (a) and the top curve in (b) are magnified by five and three times, respectively.

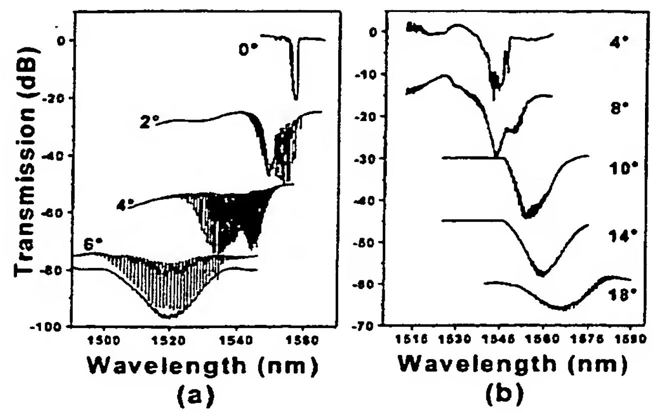

Fig. 3. Transmission-loss profiles of two sets of BFBGs in MMF fabricated using (a) phase-mask and (b) holographic techniques. Note: the smoother curve in the bottom plot of (a) is the profile of the grating immerged in index-matching gel.

which maximum radiation loss occur shift in opposite directions with increasing tilt angle for blazed gratings fabricated by both methods. The increasing tilting angle induced movement tendency of Bragg and radiation responses observed in the experiment is in excellent agreement with the modeling results shown in Fig. 1(d). It should be pointed out that in order to eliminate the resonant features of the transmission profiles, caused by the cladding-mode coupling effect, the gratings were immersed in index-matching gel to mimic an infinite cladding layer; smooth radiation profiles were, thus, obtained. However, it was noted that the transmission profiles of blazed gratings made by the holographic method were relatively smoother [as shown in Fig. 2(b)] than those written using the phase-mask method when measured in air. This profile smoothing effect results from the slightly chirped structure of the gratings introduced by the somewhat diverging UV beam used in the holographic system during the fabrication.

Fig. 3(a) and (b) shows typical transmission-loss profiles for two sets of BFBGs produced in MMF by the phase-mask and the holographic methods, respectively. The profiles were measured without immersing the gratings in index-matching gel. Distinct cladding-mode coupling features (a comb-like resonance) are apparent on the profiles of the gratings made by the phase-mask technique. As with the SMF gratings, there is a profile-smoothing effect on the blazed gratings fabricated using the holographic technique. Although in general gratings in MMF show a similar tilt-angle induced spectral profile evolution to SMF, the radiation-mode out-coupling is significantly stronger and more spectrally confined in MMF than in SMF. For example, gratings with a 10° tilt angle produced by the holographic technique achieved a maximum radiation out-coupling of 14 dB with a 10-nm (measured at 3-dB positions) dynamic range in MMF compared with only 4.5 dB with 15 nm in SMF. The strong radiation-mode out-coupling in MMF is expected since MMF has a much larger core (50 μm) which covers more tilted fringes than SMF does, thus resulting in stronger wavelength-selective radiation out-coupling.

III. Side Detection of Radiation Power Distribution

If radiation-mode out-coupling can be detected from the grating position within the fiber, an optical spectrum analyzer function may be easily implemented. This function is of

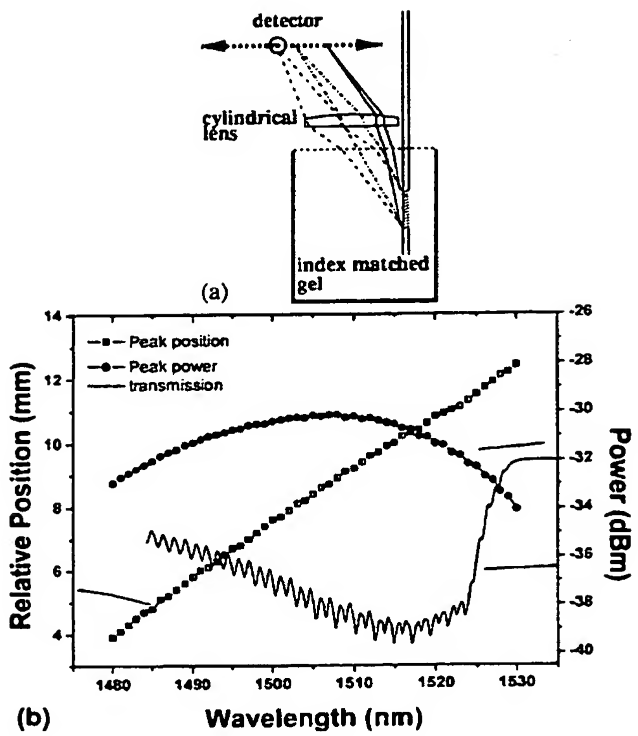

Fig. 4. (a) Schematic diagram of the side detection of BFBG. (b) Plots of peak power of radiation out-coupling against wavelength (top curve) measured by side detection, transmission-loss profile (bottom curve) measured by end detection, and spatial-to-spectral relationship (squared curve) for a BFBG with an external tilt angle of 6°.

enormous utility since it offers an easy implementation method for low-cost WDM devices for applications in telecommunications and optical sensing. To this end, we have performed an experiment to side-detect the radiation-mode out-coupling from blazed gratings using a side-detection system as sketched in Fig. 4(a). Previous papers [3], [7] and our theoretical study show that the directional radiation-mode out-coupling is strongly polarization dependent and is significantly weakened at large blaze angles. Thus, we chose a grating with a relatively small tilt angle (6°) for initial investigation. To eliminate the cladding-mode coupling effect, we immersed the grating in index-matching gel. A cylindrical lens was used to focus the light on to the detector. The detector was mounted on a motorized translation stage and used to scan the spatial distribution of the radiated light at distinct wavelengths, output from a tunable laser.

The measured radiation power peaks along the x axis (along which the detector moves) for different wavelengths are shown in Fig. 4(b). When the wavelength of the injected light changes, the corresponding focus point on the x axis moves, giving a clear spatial-to-spectral relationship. The squared curve in Fig. 4(b) plots the peak power position against the wavelength, exhibiting a linear characteristic with a conversion coefficient of 0.17 mm/nm. The top and bottom curves in Fig. 4(b) are the radiation-mode out-coupling profiles from side detection and from end detection, respectively. The dissimilar shapes and center positions of these two curves are caused for the main part by the non-normalized side-detection measurement. The normalization of the side-detected radiation-mode profile could be realized if the radiation power was measured from both y and x direction.

IV. Conclusion

We have fabricated and fully characterized BFBGs in SMF and MMF-inscribed using both phase-mask and holographic writing techniques. Comparative characterization reveals that the radiation-mode out-coupling is significantly stronger and spectrally more confined for blazed gratings in MMF than those in SMF. More importantly, we demonstrated that the radiation-mode out-coupling can be effectively measured from the physical grating position within the fiber using the side-detection technique with a high spatial–spectral resolution (0.17 mm/nm). This spatial-to-spectral encoding function of BFBGs could be exploited for low-cost WDM devices and applications in telecommunications and optical sensing.

Acknowledgment

The authors would like to thank BAE Systems, Indigo Photonics Ltd., and Deutsch Ltd. for their technical support and useful discussions.

References

[1] R. S. Westbrook, K. S. Feder, P. I. Reyes, P. Steinvurzel, B. J. Eggleton, R. G. Ernst, L. A. Reith, and D. M. Gill, "Application of fiber Bragg grating filter/tap module to a wavelength-locked low-chirp directly-modulated 10 Gb/s RZ transmitter," presented at the *OFC*, Anaheim, CA, 2002, Paper ThGG49.

[2] R. Kashyap, R. Wyatt, and R. J. Campbell, "Wideband gain flattened erbium fiber amplifier using a photosensitive fiber blazed grating," *Electron. Lett.*, vol. 29, no. 2, pp. 154–156, 1993.

[3] H. Labidi, C. Debarros, R. Letteron, and I. Riant, "Slanted Bragg grating with ultra-low polarization dependant loss," presented at the *OFC*, Anaheim, CA, 2002, Paper TuQ5.

[4] Y. Liu, L. Zhang, and I. Bennion, "Fabricating fiber edge filters with arbitrary spectral response based on tilted chirped grating structures," *Meas. Sci. Technol.*, vol. 10, pp. L1–L3, 1999.

[5] S. J. Mihailov and R. B. Walker, "Fabrication of tilted grating-grating polarization-dependent loss equalizer," *Electron. Lett.*, vol. 37, no. 5, pp. 284–286, 2001.

[6] T. Erdogan and J. E. Sipe, "Tilted fiber phase gratings," *J. Opt. Soc. Amer. A*, vol. 13, no. 2, pp. 296–313, 1996.

[7] Y. Li, M. Froggatt, and T. Erdogan, "Volume current method for analysis of tilted fiber gratings," *J. Lightwave Technol.*, vol. 19, pp. 1580–1591, Oct. 2001.